Monophotonic Ionization of 7-Azaindole, Indole, and Their Derivatives and the Role of Overlapping Excited States

F. Gai, R. L. Rich, and J. W. Petrich*

Contribution from the Department of Chemistry, Iowa State University, Ames, Iowa 50011

Received July 8, 1993®

Abstract: 7-Azaindole undergoes monophotonic ionization just as its counterpart, indole. This result suggests that 7-azaindole is qualitatively more similar to indole than has previously been recognized. The appearance of the solvated electron for zwitterionic and anionic 7-azatryptophan and for 7-azaindole in water and methanol is complete within 1 ps, which indicates that the fluorescent state whose lifetime is >100 ps cannot be the source of the electron. The origin of the electron is related to the presence of closely spaced or overlapping excited states in 7-azaindole, which is another similarity that this chromophore bears with respect to indole. The fluorescence quantum yield of 7-azaindole is shown to be excitation wavelength dependent. The excitation-wavelength dependence and the temperature dependence of the fluorescence quantum yield of 7-azaindole are explored and related to the production of the solvated electron. The implications of these observations for the use of 7-azatryptophan as an alternative to tryptophan as a probe of protein structure and dynamics are discussed.

Introduction

7-Azaindole is the chromophoric moiety of the nonnatural amino acid, 7-azatryptophan, which we have proposed as an alternative to tryptophan as an optical probe of protein structure and dynamics[1-4] (Figure 1). One observation that renders 7-azatryptophan preferable to tryptophan as an optical probe is that its fluorescence lifetime over most of the pH range is single exponential when emission is collected over the entire band.[2,5] On the other hand, the fluorescence lifetime of tryptophan at neutral pH is nonexponential.[6] Characterization of the 7-azaindole chromophore as an optical probe requires an understanding of its nonradiative pathways of deactivation.

We have reported the monophotonic production of solvated electrons in 7-azaindole.[5] This observation is particularly intriguing because it indicates that its photophysics is more similar to those of indole, which also undergoes monophotonic ionization,[7] than had previously been recognized. In fact, it is the ability of the indole moiety of tryptophan to undergo excited-state charge transfer to side-chain acceptors at various separation distances that has been suggested as the explanation for the nonexponential fluorescence decay in tryptophan.[6] A fundamental question, then, is if photoionization is also a significant nonradiative process in 7-azatryptophan, why is its fluorescence decay a single exponential of 780 ps?[1,2] In order to begin to address this question, in this article we discuss the monophotonic ionization of the 7-azaindole chromophore in detail, and we relate this ionization to the excited-state manifold of 7-azaindole.

The arguments and conclusions that will be presented here depend on several diverse observations of the photophysics of indole and 7-azaindole. We summarize them here.

1. Indole in water and methanol, 7-azaindole in water and methanol, 5-methoxyindole in water (methanol was not used as a solvent), and their analogs (investigated mostly in water) photoionize monophotonically and instantaneously to produce the solvated electron.[5,7,8] Unless otherwise indicated, the results reported here are obtained using water as the solvent. Because the fluorescent state of these analogs is always characterized by an average lifetime of at least hundreds of picoseconds, the solvated electron cannot originate from the lowest excited singlet.

2. Fluorescence-excitation anisotropy spectra of 7-azaindole in propylene glycol glasses indicate, as for indole,[3,9] the presence of closely spaced ^1L_a and ^1L_b electronic states in 7-azaindole whose transition dipole moments are at large angles to each other.[3]

3. We demonstrate here that the fluorescence quantum yields, ϕ_F, of indole, 7-azaindole, and 5-methoxyindole, are all strongly dependent on excitation wavelength.

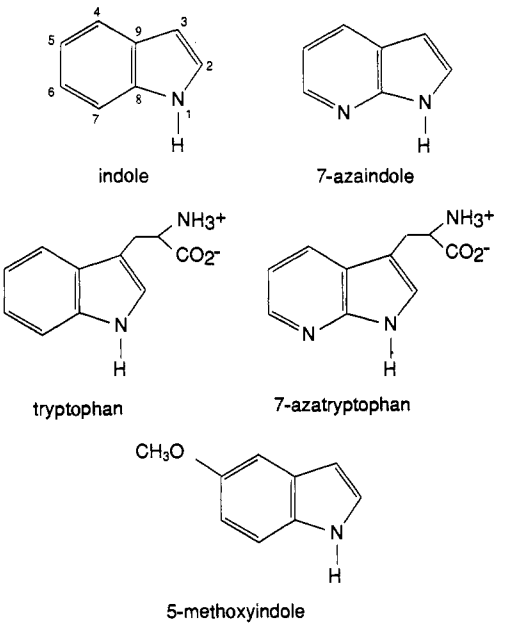

Figure 1. Structures of indole, 7-azaindole, zwitterionic tryptophan, zwitterionic 7-azatryptophan, 5-methoxyindole.

* To whom correspondence should be addressed.

® Abstract published in *Advance ACS Abstracts*, January 1, 1994.

(1) Négrerie, M.; Bellefeuille, S. M.; Whitham, S.; Petrich, J. W.; Thornburg, R. W. *J. Am. Chem. Soc.* **1990**, *112*, 7419.

(2) Chen, Y.; Rich, R. L.; Gai, F.; Petrich, J. W. *J. Phys. Chem.* **1993**, *97*, 1770.

(3) Rich, R. L.; Chen, Y.; Neven, D.; Négrerie, M.; Gai, F.; Petrich, J. W. *J. Phys. Chem.* **1993**, *97*, 1781.

(4) Rich, R. L.; Négrerie, M.; Li, J.; Elliott, S.; Thornburg, R. W.; Petrich, J. W. *Photochem. Photobiol.* **1993**, *58*, 28.

(5) Gai, F.; Chen, Y.; Petrich, J. W. *J. Am. Chem. Soc.* **1992**, *114*, 8343.

(6) Petrich, J. W.; Chang, M. C.; McDonald, D. B.; Fleming, G. R. *J. Am. Chem. Soc.* **1983**, *105*, 3824.

(7) Bent, D. V.; Hayon, E. *J. Am. Chem. Soc.* **1975**, *97*, 2612.

(8) Négrerie, M.; Gai, F.; Lambry, J.-C.; Martin, J.-L.; Petrich, J. W. *J. Phys. Chem.* **1993**, *97*, 5046; Négrerie, M.; Gai, F.; Lambry, J.-C.; Martin, J.-L.; Petrich, J. W. In *Ultrafast Phenomena VIII*; Martin, J.-L., Migus, A., Eds.; Springer: New York, 1993; p 621.

(9) Valeur, B.; Weber, G. *Photochem. Photobiol.* **1977**, *25*, 441.

0002-7863/94/1516-0735$04.50/0

Table 1. Fluorescence Quantum Yields[a]

compound	λ_{abs}^{max} (nm)	ϕ_F^{max} [b]	ϕ_F (literature)[c]
indole	270	0.45 ± 0.05 (270 nm)	0.45 [13,20], 0.27 [21], 0.23 [18]
tryptophan	278	0.18 ± 0.01 (280 nm)[d]	0.13 [14], 0.12 [15], 0.2 [16], 0.14 [17,18], 0.06 [19]
7-azaindole	289	0.056 ± 0.007 (265 nm)	0.03 [20]
5-methoxyindole	270	0.43 ± 0.02 (260 nm)	0.22 [21]

[a] Data reported from our laboratory were obtained at 24.5 ± 0.5 °C. [b] The fluorescence quantum yield measurements were performed by varying the excitation wavelength in increments of 5 nm. The excitation wavelength that yields the maximum fluorescence quantum yield is therefore only approximate. [c] These quantum yield values were obtained over a range of 23–27 °C or simply at "room temperature." We assume that most of these measurements were made at the absorbance maxima since excitation wavelengths are not given in the references. For purposes of comparison, we note that at the absorbance maxima of indole (270 nm) and of 7-azaindole (290 nm), we obtain fluorescence quantum yields of 0.45 ± 0.05 and 0.039 ± 0.002, respectively. [d] The wavelength dependence of the fluorescence quantum yield of zwitterionic tryptophan was not investigated for this work. The value we report here was determined at 280 nm.

4. The excitation-wavelength dependence of ϕ_F is used to assign the ^1L_b state to the photoionizable channel in these compounds.

5. In zwitterionic tryptophan, the presence of the $-NH_3^+$ and $-CO_2^-$ side-chain groups brings considerable complexity to the indolyl photophysics. In particular, nonexponential fluorescence decay is observed.[6] These side chains are not, however, a source of nonexponential fluorescence decay in zwitterionic 7-azatryptophan.[1,2]

We argue that these data can be synthesized and comprehended by the following working *hypotheses*.

1. The ^1L_b state is photoionizable, and the ^1L_a state is not.

2. The ^1L_a state is coupled to charge-transfer states, which are the source of the nonexponential fluorescence decay in tryptophyl derivatives.

3. Wave packet evolution away from the initial Franck–Condon region provides a means of rationalizing these data.

With this summary in mind, we shall now present and discuss our results in more detail.

Experimental Section

7-Azaindole (7AI) (Sigma) was purified by flash chromatography[2,11] using ethyl acetate as a solvent. Indole, tryptophan (Trp), D,L-7-azatryptophan (7AT), 5-hydroxytryptophan (Sigma), 5-methoxyindole (5MeOI) (Aldrich), stilbene (Sigma), rhodamine B (Eastman Kodak Co.), *p*-terphenyl (Sigma), and quinine sulfate monohydrate (Aldrich) were used without further purification. N_1-methyl-7-azaindole (1M7AI) and 7-methyl-7*H*-pyrrolo[2,3-*b*]pyridine (7M7AI) were prepared as described elsewhere.[2]

For steady-state anisotropy determinations, all compounds were dissolved in propylene glycol, and experiments were performed as discussed previously.[3] Stilbene was used as a reference compound because it has been reported to have a limiting anisotropy of 0.4.[12]

Quantum yield determinations were performed as outlined by Teale and Weber[13] and by Chen.[14] Previous work[65] has demonstrated that Beer's law is valid for indole at these concentrations. We assume the same holds true for the other species in this study. Quinine sulfate and *p*-terphenyl were used as standards. Verification of our experimental setup and quantum yield calculations was performed using rhodamine B in ethylene glycol. We examined the wavelength regions, 530–570 nm, where excitation into the first excited-state singlet occurs for rhodamine B and the ultraviolet region, 240–320 nm, where the indoles absorb. Because the fluorescence quantum yield of quinine sulfate is excitation-wavelength dependent,[66] all our analyses, therefore, are relative to the quantum yield of quinine sulfate in 1.0 N H_2SO_4, which is 0.55 at λ_{ex} = 348 nm.[14] We observe the fluorescence quantum yield of rhodamine B to be 0.98 ± 0.05 at λ_{ex} = 555 nm. This quantum yield deviates less than 5% over the visible range of excitation wavelengths we employed (Figure 5d). The deviation in the quantum yield using ultraviolet excitation wavelengths (240–320 nm) was more significant (20%), but this may be due to the low absorbance of rhodamine B in this region as well as to impurities. Literature values for rhodamine B are 0.89 in ethylene glycol and 0.97 in ethanol.[13] If we do not include a correction for the refractive indices of the rhodamine B and quinine sulfate solutions (outlined below), we obtain a quantum yield of 0.88 at λ_{ex} = 555 nm for rhodamine B.

As an additional check of our procedures, we determined the fluorescence quantum yield of zwitterionic tryptophan by comparison to the quantum yield of another known standard, *p*-terphenyl (ϕ_F = 0.93[67]). A range of values has been reported (0.06–0.20[14–19]). Using an excitation wavelength of 280 nm, we obtain a fluorescence quantum yield of 0.18 ± 0.01 for zwitterionic tryptophan.

Indole, 7-azaindole, and 5-methoxyindole were dissolved in water. The quantum yield data listed in Table 1 of each compound were determined relative to quinine sulfate.

Sample temperature was controlled with a M9000 Fisher refrigerated circulator connected to the cell holder and monitored directly at the sample by an HH-99A-T2 Omega thermocouple. Absorbance measurements were made using a Shimadzu UV-2101PC double-beam spectrophotometer. Steady-state fluorescence measurements were made using a Spex Fluoromax. All spectra were corrected for fluctuations in lamp intensity and detector response. A 0.6–4-nm band-pass was used for excitation and emission, depending on the quantum yield of each compound. For samples of high quantum yield, narrow slit widths are required to prevent signal saturation of the detector. We ensure that signal saturation does not occur for a given slit width by comparing the emission spectra of solutions having a range of concentrations within Beer's law. If the emission intensity decreases proportionally to the dilution factor and the spectral shape does not change, saturation does not occur.

The excitation-wavelength dependence of the fluorescence quantum yield of the indoles (Figures 5a–c) is a significant observation whose novelty required the investigation of many possible artifacts. Most significant is the possible reabsorption at the reddest excitation wavelengths when samples of high concentration are required. (Three solutions of various sample concentration ($0.05 \leq OD(\lambda_{ex}) \leq 0.15$) were prepared for each excitation wavelength examined in order to measure accurately the sample absorbance or to prepare a solution giving a large enough fluorescence signal.) This proved to be important in the rhodamine B analysis (since there is significant overlap between the absorption and emission spectra) but an almost negligible factor for the indoles. The true fluorescence quantum yield is given by (where $\bar{\nu}$ is the energy in wavenumbers, $I^{obs}(\bar{\nu})$ is the observed fluorescence spectrum, and A is the optical density)

$$\phi_F = \int_{-\infty}^{+\infty} I(\bar{\nu})d\bar{\nu} = \int_{-\infty}^{+\infty} I^{obs}(\bar{\nu})10^{A(\bar{\nu})}d\bar{\nu}$$

$$\simeq \int_{-\infty}^{+\infty} I^{obs}(\bar{\nu})[1 + 2.303A(\bar{\nu})]d\bar{\nu}$$

The correction was never more than 7%, and then only for rhodamine B at λ_{ex} = 570 nm.

Another correction was possible inner filter effects,[68] which arise from not collecting all the fluorescence emitted from the sample. In our analyses, this inner filter effect does not occur since the fluorimeter sample cell holder blocks no portion of the cuvette face.

Corrections for the differences in the indices of refraction between two solvents were also considered. Such a correction affects the absolute quantum yield determined for each sample but does not change the excitation-wavelength dependent profile of an individual species. The quantum yields are corrected using the relationship:[69] $\phi_F = \phi_F^{uncorr}[n(s)^2/n(r)^2]$, where $n(s)$ and $n(r)$ are the refractive indices at the emission wavelengths of interest of the sample solvent and reference solvent, respectively. In our experiments, the correction was 11% for rhodamine B in ethylene glycol compared to quinine sulfate in water. Since the refractive index of water changes less than 2% from 300 to 589 nm[70]

(10) Eftink, M. R.; Selvidge, L. A.; Callis, P. R.; Rehms, A. A. *J. Phys. Chem.* **1990**, *94*, 3469.
(11) Still, W. C.; Kahn, M.; Mitra, A. *J. Org. Chem.* **1978**, *43*, 2923.
(12) Ruggiero, A. J.; Todd, D. C.; Fleming, G. R. *J. Am. Chem. Soc.* **1990**, *112*, 1003.
(13) Teale, F. W. J.; Weber, G. *Trans. Faraday Soc.* **1957**, *53*, 646.
(14) Chen, R. F. *Anal. Lett.* **1967**, *1*, 35.

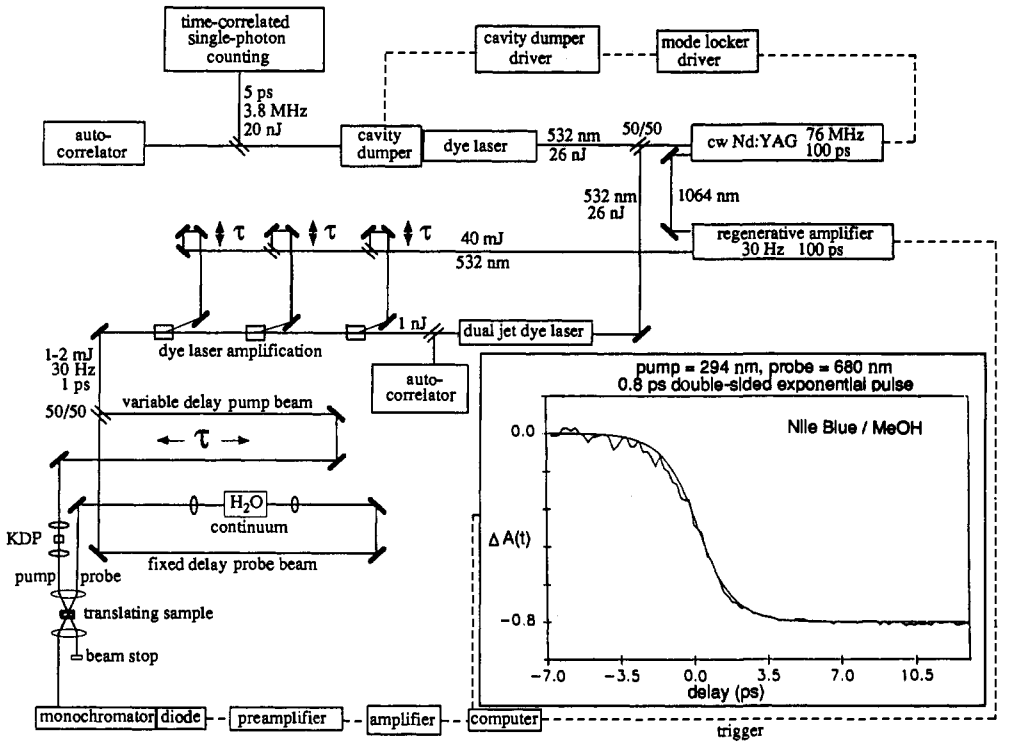

Figure 2. Experimental apparatus for pump-probe transient absorption measurements. Also displayed (inset) is the rise time of the induced bleaching of nile blue in methanol, $\lambda_{ex} = 294$ nm, $\lambda_{probe} = 680$ nm. The amplified laser pulse width is deconvoluted from the molecular response and is best described by a double-sided exponential of 0.8 ps full width at half-maximum.

(1.358–1.329), and since the emission spectra of the indoles do not change with excitation wavelength, no correction for the index of refraction was required in comparing the fluorescence quantum yield at one excitation wavelength with respect to another.

We investigated the possibility that the variations in the plots of ϕ_F vs λ_{ex} resulted from absorption by excited-state transients such as solvated electrons or triplets. For example, the extinction coefficient for a solvated electron (ϵ_{e^-}) is about 1000 M^{-1} cm^{-1} at 400 nm (and *decreases* toward higher energies).[28] If we take the *extreme* case and assume that all of the ground-state population is projected into the excited state and if we take the quantum yield of photoionization as 0.2, then the maximum correction for absorption by electrons is less than 1%. Under normal conditions of excitation, the absorption by solvated electrons is insignificant. Similarly, the contribution due to absorption by triplets should be even smaller.

The fluorescence excitation spectra of indole, 7-azaindole, and 5-methoxyindole in water all differ from their respective absorption spectra. The differences are largest in 5-methoxyindole. In indole and 7-azaindole, the differences are small but reproducible. It is important to recognize that the magnitude of the difference between a fluorescence excitation spectrum and an absorption spectrum can be greatly *underestimated* because in order to compare the two *they must be normalized.* (A change between the two spectra will also be underestimated—or annulled—by normalization if it occurs in a region where the spectra change rapidly with wavelength, as occurs on the red edges of the indole spectra.) This normalization usually takes the form of setting the value of the optical density and the fluorescence intensity to be arbitrarily equal at a given wavelength.

As a final indication of self-consistency, we note that curves similar to the ones displayed in Figure 5a–c can be constructed directly from the excitation spectra. If the emission spectral shape does not change with respect to excitation wavelength (we do not observe such a change), then the integrated area of the emission (the fluorescence quantum yield) is proportional to the emission intensity. When the fluorescence intensity at a given emission wavelength is monitored in order to obtain an excitation spectrum, the quantum yield over the range of excitation wavelengths is essentially what is observed *if for each fluorescence intensity measured an accurate correction is made for the sample absorbance.* Such a correction is similar to that used to obtain standard quantum yields, except that no factor to account for the fluorimeter lamp intensity is included since this has already been accounted for when obtaining the excitation spectrum itself. Of course, if the absorption and excitation spectra are *exactly* superimposable, this procedure yields a plot of the quantum yield that is independent of the excitation wavelength.

Fluorescence lifetime measurements were performed with the time-correlated single-photon counting apparatus described elsewhere.[2] In the course of this article, we make a distinction between anisotropies obtained from two types of experiments: r_0 is the anisotropy obtained from steady-state, low-temperature measurements; $r(0)$ is the limiting anisotropy obtained from time-dependent measurements in the liquid phase.[3]

Pump–probe transient absorption measurements were performed with a system based on an Antares 76s cw-modelocked Nd:YAG synchronously pumping a Coherent 701-2 dye laser with 1 W of 532-nm radiation (Figure 2). The output of the dye laser was amplified to 1–2 mJ at 30 Hz with a Continuum regenerative amplifier that is seeded with residual 1064-nm radiation from the Antares. Half of the amplified dye-laser pulse train is focused into a cell containing water to form a white light continuum that is used as a probe beam. The remainder of the pulse train is focused into a crystal of KDP to obtain the appropriate ultraviolet wavelength for excitation.

The pulsewidth of the amplified pulse train is determined by measuring the apparent rise time of the induced transmission or absorption of a standard (Figure 2). In the pump-probe experiments discussed here, the typical full scale is 800 ps. It is thus crucial that the translation stage (optical delay line) is adequately aligned so as to avoid drift in the overlap of the pump and probe beams during the course of the experiment. Our

(15) Børrensen, H. C. *Acta Chem. Scand.* **1967**, *21*, 920.
(16) Weber, G.; Teale, F. W. J. *Biochem. J.* **1957**, *65*, 476.
(17) Eisenger, J. *Photochem. Photobiol.* **1969**, *9*, 247.
(18) Eisenger, J.; Navon, G. *J. Chem. Phys.* **1969**, *50*, 2069.
(19) Shore, V. G.; Pardee, A. B. *Arch. Biochem. Biophys.* **1956**, *60*, 100.
(20) Avouris, P.; Yang, L. L.; El-Bayoumi, M. A. *Photochem. Photobiol.* **1976**, *24*, 211.
(21) Klein, R.; Tatischeff, I. *Chem. Phys. Lett.* **1977**, *51*, 333.
(22) Lin, S. H.; Fujimura, Y.; Neusser, H. J.; Schlag, E. W. *Multiphoton Spectroscopy of Molecules*; Academic Press: New York, 1984.
(23) Wiesenfeld, J. M.; Ippen, E. P. *Chem. Phys. Lett.* **1980**, *73*, 47.
(24) Bobrovich, V. P.; Sarzhevskii, A. M.; Senyuk, M. A. *Zh. Prikl. Spektrosk.* **1978**, *30*, 1022.
(25) Feitelson, J. *Photochem. Photobiol.* **1971**, *13*, 87.
(26) Robbins, R. J.; Fleming, G. R.; Beddard, G. S.; Robinson, G. W.; Thistelthwaite, P. J.; Woolfe, G. J. *J. Am. Chem. Soc.* **1980**, *102*, 6271.
(27) Kirby, E. P.; Steiner, R. F. *J. Phys. Chem.* **1970**, *74*, 4480.
(28) Hart, E. J.; Anbar, M. *The Hydrated Electron*; Wiley-Interscience: New York, 1970. Data from this text for the extinction coefficient of the solvated electron at 650 nm in units of M^{-1} cm^{-1} can be plotted against temperature and fit very well to a straight line. We obtain $\epsilon(T) = 1750 - 66.5T(°C)$.

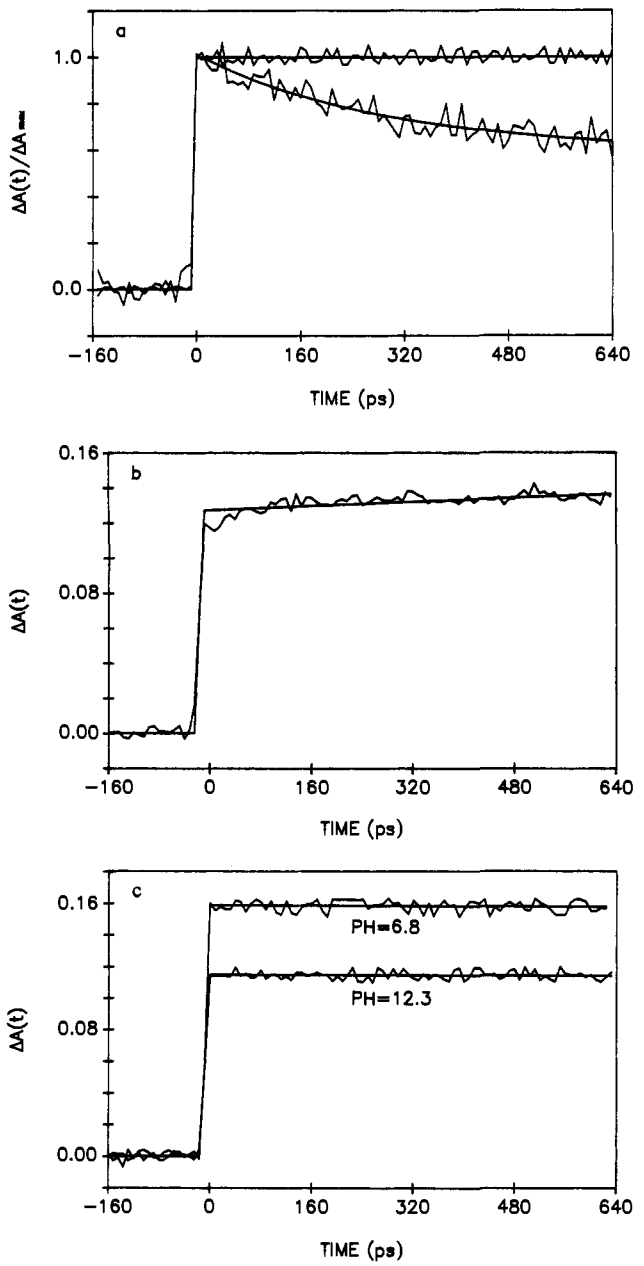

Figure 3. Transient absorption arising from the solvated electron at 23 °C. (a) Zwitterionic tryptophan, pH 6.8; λ_{ex} = 304 nm, λ_{probe} = 650 nm. The *decaying* signal is obtained in the presence of 0.25 M KNO_3. The upper trace is flat on the time scale of the measurement. The maximum absorption change in the absence of scavenger is 0.16; in the presence of 0.25 M KNO_3, it is 0.05. The two traces are normalized to have the same maximum absorption change. Similar behavior is observed for 7AI, 1M7AI, and 7M7AI. (b) Tryptophan, pH 12.3; λ_{ex} = 294 nm, λ_{probe} = 580 nm. The data are fit to 10% of a rising component of duration 3.2 ns. Identical results are obtained with λ_{ex} = 304 nm. This rise time is identical to the value of the single-exponential decay time we obtain for tryptophan at pH 12.3 by means of time-correlated single-photon counting. (c) Zwitterionic 7-azatryptophan, pH 6.8, and anionic 7-azatryptophan, pH 12.3; λ_{ex} = 294 nm, λ_{probe} = 580 nm. Identical results are obtained using an excitation wavelength of 304 nm.

system was thus regularly aligned by reproducing the "flat" transient absorbance of the solvated electron produced from zwitterionic tryptophan or 7-azatryptophan (Figure 3). Geminate recombination of the electron does not occur on this time scale.[8]

The quantum yield of photoionization was determined at various excitation wavelengths using the relation

$$\Delta A_{e^-} = \epsilon_{e^-} l c_{e^-} = \epsilon_{e^-} l \phi_{e^-} I_{abs} \rho$$
$$= \rho \epsilon_{e^-} l \phi_{e^-} I_0 (1 - 10^{-A_{e^-}}) \quad (1)$$

where ϵ_{e^-} is the extinction coefficient of the solvated electron at the probe wavelength, l is the sample pathlength, c_{e^-} is the concentration of the solvated electron, ρ is a constant that is proportional to the overlap between pump and probe pulses, ϕ_{e^-} is the quantum yield of the solvated electron, and A_{e^-} is the optical density of the sample at the pump wavelength.

A similar expression can be obtained for the change in optical density for a reference molecule, such as nile blue (Figure 2):

$$|\Delta A_N| = \rho \epsilon_N l I_0 (1 - 10^{-A_N}) \quad (2)$$

The absolute value sign is used because nile blue provides a transient bleaching instead of absorption. We are only concerned here in normalizing the optical density changes. It follows that

$$\phi_{e^-} = \frac{\Delta A_{e^-}(1 - 10^{-A_N})\epsilon_N}{\Delta A_N (1 - 10^{-A_{e^-}})\epsilon_{e^-}} \quad (3)$$

Table 2. Solvated Electron Yield (ϕ_{e^-}) vs Excitation Wavelength (λ_{ex})[a]

	excitation wavelength (nm)			
compound	294	301	303	305
Trp (pH 6.5)	0.14 ± 0.05	0.43 ± 0.05	0.35 ± 0.03	0.31 ± 0.08
7AI (pH 6.9)	0.08 ± 0.03	0.16 ± 0.04	0.14 ± 0.03	0.15 ± 0.04
5MeOI (pH 7.3)	0.23 ± 0.04			0.27 ± 0.02

[a] The probe wavelength for all measurements is 665 nm. At this wavelength the extinction coefficient for the reference compound, nile blue in ethanol, is approximately equal to that of the solvated electron: 1.8×10^4 M^{-1} cm^{-1}. All measurements were performed at 23 °C. The absence of a value indicates that the measurement was not performed.

Results

A. Monophotonic Ionization. The flash photolysis studies of indole and tryptophan by Bent and Hayon[7] are a natural point of comparison for our work on 7-azaindole. Bent and Hayon observed that for tryptophan a logarithmic plot of the absorbance of the solvated electron against the photolyzing pump intensity gave a straight line of slope 1.25 at pH 7.5. This result is consistent with monophotonic ionization.[22] Nevertheless, the electron appeared within their pulsewidth of 3.6 ns, leading them to suggest that an electronic state higher than S_1 or that a hot vibrational state of S_1 was the ionizing species. For tryptophan they observed that the zwitterion produced the solvated electron within the duration of their pump pulse; but that at pH 10.3, where the amino group is deprotonated and only the anion is present, about 10% of the solvated electron appears with a rise time equal to the ~8-ns decay time of the fluorescent species.

Figure 3 presents our results for tryptophan on a time scale of 800 ps using 1-ps pump and probe pulses. For zwitterionic tryptophan, the solvated electron appears within the duration of the pump pulse. On the other hand, at pH 12.3 where we measure the fluorescence lifetime of anionic tryptophan to be 3.17 ns, *a small amount* of the solvated electron appears with a similar rise time, just as in the earlier experiment of Bent and Hayon.

That the transient absorption in Figure 3 is due to a solvated electron is demonstrated by the transient quenching in the presence of the electron scavenger, KNO_3.[23] For 7-azaindole, the dependence of the logarithm of the absorption of the solvated electron at "zero time" upon the logarithm of the pump intensity is presented in Figure 4. The slope is 1.2 ± 0.3 indicating a monophotonic ionization.

Table 2 indicates that the quantum yield of the solvated electron is excitation-wavelength dependent for tryptophan. For 7-azaindole and 5-methoxyindole, because the electron yield is less than that in tryptophan and because of experimental error, the excitation-wavelength dependence is obscured. The data for tryptophan indicate that the electron yield is higher toward the red edge of the absorption spectrum and are thus consistent with the diminished fluorescence quantum yield at those wavelengths (Figure 5). The yields for the solvated electron production for a variety of compounds, relative to that for tryptophan, are listed in Table 3.

Table 3. Quantum Yield of Solvated Electron[a]

compound	ϕ_{e^-}	compound	ϕ_{e^-}
tryptophan, pH 6.8	1.00[b]	7M7AI (N_1), pH 12.3	0.30
indole, pH 6.4	0.86	7M7AI (N_1), pH 8.8	0.16
7AI (N_7, N_1H), pH 6.3	0.38	7M7AI (N_1H^+), pH 3.3	0.14
7AI (N_7H^+, N_1H), pH 2.1	0.16	1M7AI (N_7), pH 6.8	0.32
7AT (N_7, N_1H), pH 6.7	0.28	7AI/methanol	0.17
7AT (N_7H^+, N_1H), pH 2.1	0.12		

[a] All yields are reported relative to that of zwitterionic tryptophan at 23 °C. λ_{ex} = 304 nm, λ_{probe} = 650 nm. In all cases, the solvated electron appears within our ~1-ps pulse width. The reported values reflect an uncertainty of ~15%. See Experimental Section for abbreviations. [b] Using an excitation wavelength of 265 nm, Bent and Hayon[7] obtain an absolute quantum yield of 0.08 for the production of photoelectrons from zwitterionic tryptophan (pH 6.0) at 25 °C.

The motivation for measuring ionization yields for 7-azaindole in methanol was to determine whether the solvated electron originates from the normal or the tautomer form of 7-azaindole. If it originates from the tautomer form, the rise time for the solvated electron would be expected to be equal to the formation time for the tautomer, 140 ps. Such a rise time for the solvated electron is not observed.

B. Excited States. Low-temperature, steady-state fluorescence excitation anisotropy studies of 7-azaindole in propylene glycol indicate that, like indole,[9] its absorption spectrum is composed of two overlapping electronic transitions whose transition dipole moments are at large angles to each other. The fluorescence excitation anisotropy spectrum and the decomposed fluorescence excitation spectra of 7-azaindole are displayed in Figure 6. The measurements of Bulska et al.[47] suggested the presence of ^1L_a and ^1L_b bands in 7-azaindole.

Valeur and Weber[9] resolved the fluorescence excitation spectrum of indole into overlapping ^1L_a and ^1L_b bands at −58 °C in propylene glycol and reported the ^1L_b transition to be quite structured with maxima at 282.5 and 289.5 nm. The ^1L_a transition is broader and absorbs farther to the red than does the ^1L_b transition. At wavelengths longer than 295 nm, only absorption resulting from the ^1L_a transition is observed. The excitation anisotropy of 7-azaindole is qualitatively similar to that of indole, but it possesses less pronounced structure. Anisotropy minima at 293.5 and 300.5 nm and a relative maximum at 297.0 nm give rise to the structure in the resolved excitation spectra.

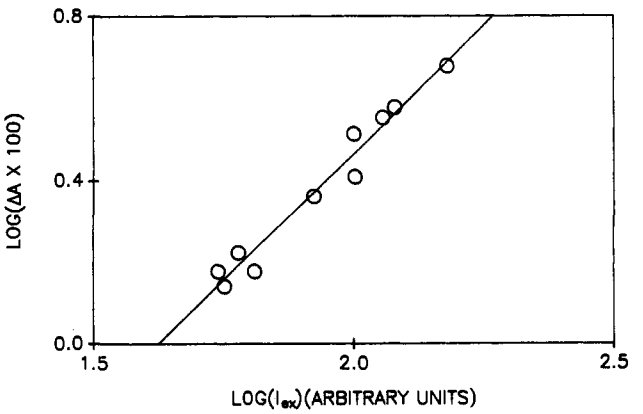

Figure 4. Plot of the logarithm of ΔA_{max} against the logarithm of the pump intensity for 7-azaindole. The plot yields a straight line with a slope of 1.2 ± 0.3, indicating a monophotonic ionization.[12]

Neither 7-azaindole, nor indole, nor 5-methoxyindole yield a limiting steady-state anisotropy, r_o, of 0.4 at any excitation wavelength. The control experiment, stilbene, produced r_o = 0.4 at $\lambda_{ex} \geq 336$ nm. Our results for stilbene are qualitatively similar to those of Bobrovich et al.,[24] who measured the excitation polarization spectrum of stilbene in butanol at 77 K.

The excitation-wavelength dependence of the photoionization process indicates that conventional methods of decomposing fluorescence excitation spectra of indole-like molecules into ^1L_a and ^1L_b absorption spectra based on measurements of polarized emission are inappropriate;[9,10] a fluorescence excitation spectrum can only be considered to represent the absorption spectrum if ϕ_F is independent of the excitation wavelength.[3]

C. Excitation Wavelength Dependence of the Fluorescence Quantum Yield. If the instantaneous appearance of the electron has its origin in the upper of the two electronic states illustrated in Figure 6b, then the fluorescence quantum yield of 7-azaindole is expected to be excitation-wavelength dependent. The data presented in Figure 5 indicate that this is the case for 7-azaindole, indole, and 5-methoxyindole. The control experiment was performed for rhodamine B in ethylene glycol, for which no excitation-wavelength dependence on the fluorescence quantum yield was observed. The observation of an excitation-wavelength dependent fluorescence quantum yield is of significance because it is consistent with the excitation-wavelength dependence of the electron yield. These two observations argue cogently, along with the log–log plot (Figure 4), for the monophotonic ionization of 7-azaindole, indole, 5-methoxyindole, and their derivatives. The photoionization of indoles has been studied extensively.[5,7,8,25,59-61] The measurements of Steen[61] and Pigault et al.[60] suggest an excitation-wavelength dependence of the electron yield, but their data are not precise enough to demonstrate that this dependence exists at wavelengths greater than 250 nm.

(29) Glasser, N.; Lami, H. *J. Chem. Phys.* **1981**, *74*, 6526.
(30) Rizzo, T. R.; Park, Y. D.; Peteanu, L.; Levy, D. H. *J. Phys. Chem.* **1986**, *84*, 2534.
(31) Rizzo, T. R.; Park, Y. D.; Levy, D. H. *J. Chem. Phys.* **1986**, *85*, 6945.
(32) Cable, J. R.; Tubergen, M. J.; Levy, D. H. *J. Am. Chem. Soc.* **1988**, *110*, 7349.
(33) Tubergen, M. J.; Cable, J. R.; Levy, D. H. *J. Chem. Phys.* **1990**, *92*, 51.
(34) Hagar, J. W.; Demmer, D. R.; Wallace, S. C. *J. Phys. Chem.* **1987**, *91*, 1375.
(35) Demmer, D. R.; Leach, G. W.; Outhouse, E. A.; Hagar, J. W.; Wallace, S. C. *J. Phys. Chem.* **1990**, *94*, 582.
(36) Arnold, S.; Sulkes, M. *J. Phys. Chem.* **1992**, *96*, 4768.
(37) Lami, H.; Glasser, N. *J. Chem. Phys.* **1986**, *84*, 597.
(38) Chen, Y.; Gai, F.; Petrich, J. W. *J. Am. Chem. Soc.* **1993**, *115*, 10158.
(39) Schowen, K. B. J. In *Transition States of Biochemical Processes*; Gandour, R. D., Schowen, R. L., Eds.; Plenum: New York, 1978; p 225.
(40) McMahon, L. P.; Colucci, W. J.; McLaughlin, M. L.; Barkley, M. D. *J. Am. Chem. Soc.* **1992**, *114*, 8442. Yu, H.-Y.; Colucci, W. J.; McLaughlin, M. L.; Barkley, M. D. *J. Am. Chem. Soc.* **1992**, *114*, 8449.
(41) Cross, A. J.; Waldeck, D. H.; Fleming, G. R. *J. Chem. Phys.* **1983**, *78*, 6455; *79*, 3173.
(42) Szabo, A. *J. Chem. Phys.* **1984**, *81*, 150.
(43) Hansen, J. E.; Rosenthal, S. J.; Fleming, G. R. *J. Phys. Chem.* **1992**, *96*, 3034.
(44) The expressions in refs 12 and 41 for I_1 and I_2 must be interchanged.
(45) Strickland, E. H.; Horowitz, J.; Billups, C. *Biochemistry* **1970**, *9*, 4914. Martinaud, M.; Kadiri, A. *Chem. Phys.* **1978**, *28*, 473. Rehms, A. A.; Callis, P. R. *Chem. Phys. Lett.* **1987**, *140*, 83. Tatischeff, I.; Klein, R.; Zemb, T.; Duquesne, M. *Chem. Phys. Lett.* **1978**, *54*, 394. Meech, S. R.; Phillips, D.; Lee, A. G. *Chem. Phys.* **1983**, *80*, 317.
(46) Waluk, J.; Pakula, B.; Komorowski, S. J. *J. Photochem.* **1987**, *39*, 49.
(47) Bulska, H.; Grabowska, A.; Pakula, B.; Sepiol, J.; Waluk, J.; Wild, U. P. *J. Lumin.* **1984**, *29*, 65.
(48) Petrich, J. W.; Longworth, J. W.; Fleming, G. R. *Biochemistry* **1987**, *26*, 2711.
(49) Tilstra, L.; Sattler, M. C.; Cherry, W. R.; Barkley, M. D. *J. Am. Chem. Soc.* **1990**, *112*, 9176. Colucci, W. J.; Tilstra, L.; Sattler, M. C.; Fronczek, F. R.; Barkley, M. D. *J. Am. Chem. Soc.* **1990**, *112*, 9182.
(50) Hogue, C. W. V.; Rasquinha, I.; Szabo, A. G.; MacManus, J. P. *FEBS Lett.* **1992**, *310*, 269.
(51) Skrabal, P.; Rizzo, V.; Baici, A.; Bangerter, Luisi, P. L. *Biopolymers* **1979**, *18*, 995. Kobayashi, J.; Higashijima, T.; Sekido, S.; Miyazawa, T. *Int. J. Pept. Protein Res.* **1981**, *17*, 486. Dezube, B.; Dobson, C. M.; Teague, C. E. *J. Chem. Soc., Perkin Trans. 2* **1981**, 730.
(52) Engh, R. A.; Chen, L. X.-Q.; Fleming, G. R. *Chem. Phys. Lett.* **1986**, *126*, 365.
(53) Szabo, A. G.; Rayner, D. M. *J. Am. Chem. Soc.* **1980**, *102*, 554.
(54) Heller, E. J. *Acc. Chem. Res.* **1981**, *14*, 368; Alvarellos, J.; Metiu, H. *J. Chem. Phys.* **1988**, *88*, 4957.
(55) Chandrasekhar, S. In *Selected Papers in Noise and Stochatic Processes*; Wax, N., Ed.; Dover: New York, 1954; p 3. Frauenfelder, H.; Wolynes, P. G. *Science* **1985**, *229*, 337.
(56) The presolvated electron is known to appear from 7-azaindole in ≤130 fs.[8] This does not, however, place an ~100-fs time scale on the event of photoionization but rather indicates a time scale for the *localization* of the photoelectron.

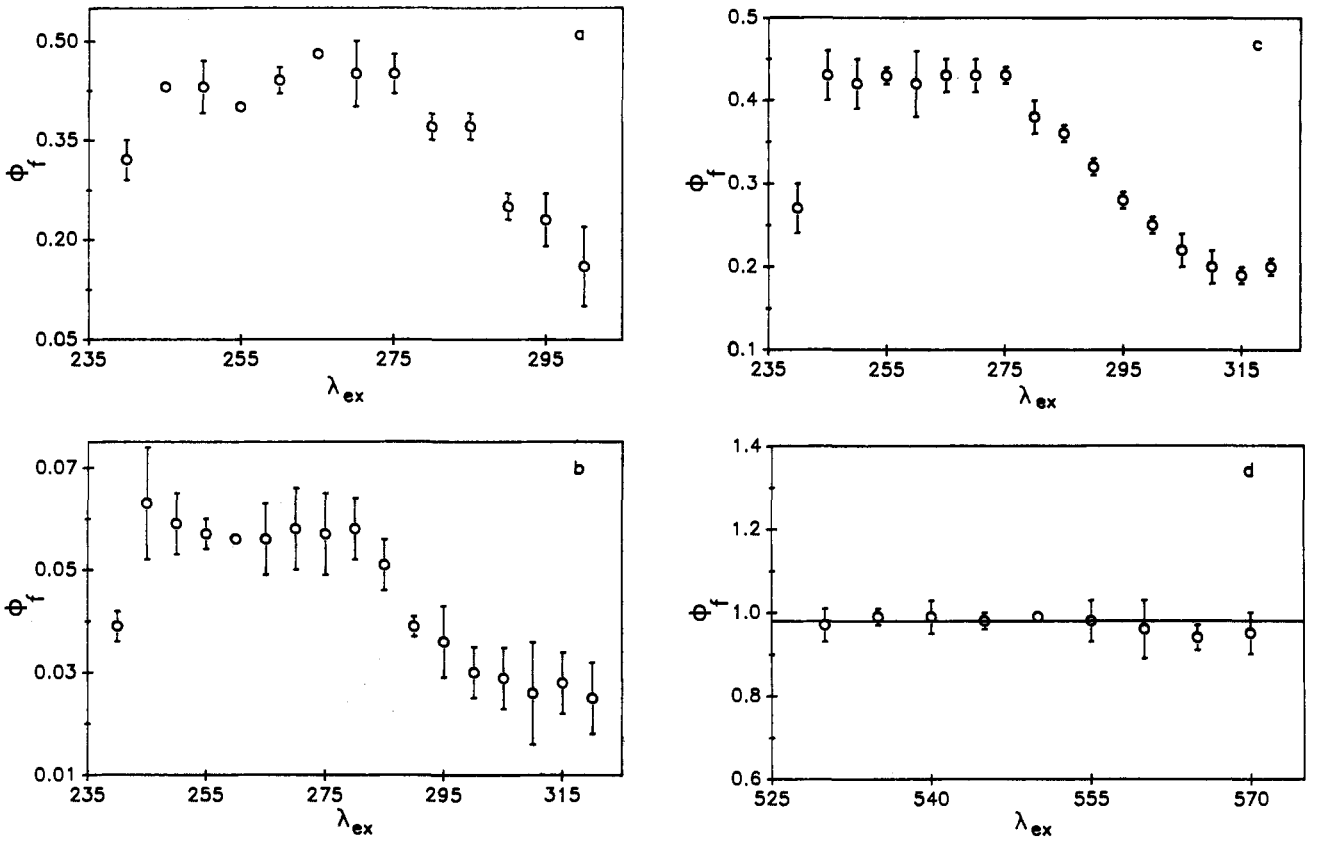

Figure 5. Fluorescence quantum yield, ϕ_F, versus excitation wavelength, λ_{ex}, at neutral pH, for (a) indole, (b) 7-azaindole, (c) 5-methoxyindole, and (d) rhodamine B (in ethylene glycol).

Discussion

A. Temperature and Excitation-Wavelength Dependence of the Fluorescence Quantum Yield. The low-temperature fluorescence anisotropy data indicate the presence of closely spaced excited states in indole, 7-azaindole, and their derivatives. The instantaneous appearance of the solvated electron indicates that at least one of the excited states is dissociative. The fluorescence quantum yields of the compounds investigated here are very low at the red edge of the absorption spectrum, attain a maximum near—but usually not at—the absorption maximum, and subsequently decrease toward the blue edge of the absorption spectrum. This is in contrast to the fluorescence lifetime, which we observe to be constant over the range of wavelengths accessible to our laser system (285–310 nm). For example, our results for 7-azaindole indicate that the electron is generated monophotonically and instantaneously. A time scale of $\leq$130 fs[8,56] is required for the electron to become "solvated". The excitation-wavelength dependent fluorescence quantum yield, $\phi_F(\lambda)$, is correspondingly diminished by the instantaneous production of electrons. This is especially clear in the case of indole and tryptophan (Figure 5 and Table 2). The wavelength dependence of ϕ_F and ϕ_{e^-} led us to investigate the role of both temperature and excitation wavelength on ϕ_F and ϕ_{e^-}. These measurements were performed to address the following questions. Assuming that the variation in ϕ_F arises only from changes in the yield of solvated electrons, by performing measurements of the fluorescence quantum yield as a function of both excitation wavelength and of temperature, can we obtain any information concerning the barrier—if there is one—to photoionization? Alternatively, can we obtain any information concerning the interaction of bound and dissociative excited-state surfaces?

Our experiences were based on the suggestions in the literature that photoionization is a thermally activated process.[7,25,26] It is possible (as opposed to the case illustrated in Figure 11a) that one dissociative surface intersects the bound state near its minimum (no barrier); and the other, at a higher energy (large barrier). Alternatively, because the Franck–Condon factors for predissociation are favorably only for the vibrational levels of the bound state that coincide with the crossing of the dissociative state, the rate of photoionization increases at both low and high excitation energies (Figure 11a). The former scheme predicts that excitation to vibrational levels lying between the two crossing points will yield solvated electrons with different activation energies depending on the energy separation between the initially excited vibrational level and the upper crossing point.

The data compiled in Table 4 indicate, however, that the Arrhenius parameters are essentially independent of excitation wavelength—although some fluctuations are observed for indole. The treatment of these temperature and excitation-wavelength dependent data is as follows. Because the solvated electron is produced on a time scale that is instantaneously compared to steady-state or conventional time-correlated single-photon counting experiments, the apparent fluorescence quantum yield obtained in either of these two latter experiments must be corrected by the electron yield at "zero time"; thus,

(57) The choice of the values for $g^a(\lambda)$ is motivated by mathematical and physical necessity. The overall population decay, $K(t,\lambda)$ (eq 17), obtained at a given emission wavelength, will only be double exponential, as measured,[12] if $g^a(\lambda) \neq g^b(\lambda)$. This requirement is a consequence of the assumption that $k^a = k^b$ (eq 9). Given this, the resulting expressions from eqs 12 and 13, when substituted in eq 18, provide $\alpha_2 = 0$, that is $K(t)$ decays as a single exponential if $g^a(\lambda) = g^b(\lambda)$.

(58) Internal conversion,[46] and N_1H proton abstraction by the solvent[29,35,38,40] are other possible, significant nonradiative pathways. As we discuss elsewhere,[2] we do not consider excited-state tautomerization to be an important nonradiative pathway for 7-azaindole in water.

(59) Mialocq, J.-C.; Amouyal, E.; Bernas, A.; Grand, D. *J. Phys. Chem.* **1982**, *86*, 3173. Santus, R.; Grossweiner, L. I. *Photochem. Photobiol.* **1972**, *15*, 101. Pailthorpe, M. T.; Nichols, C. H. *Photochem. Photobiol.* **1971**, *14*, 135. Amouyal, E.; Bernas, A.; Grand, D.; Mialocq, J.-C. *Faraday Discuss. Chem. Soc.* **1982**, *74*, 147. Kandori, H.; Borkman, R. F.; Yoshihara, K. *J. Phys. Chem.* **1993**, *97*, 9664.

(60) Pigault, C.; Hasselmann, C.; Laustriat, G. *J. Phys. Chem.* **1982**, *86*, 1755.

(61) Steen, H. B. *J. Chem. Phys.* **1974**, *61*, 3997.

Table 4. Dependence of Arrhenius Parameters on Excitation Wavelength

λ_{ex} (nm)	ϕ_F[a]	ϕ_{e^-}[b]	E_a[b] (kcal/mol)	A[b,c] (s^{-1})
		Indole		
240	0.32 ± 0.03	0.18	12.8	3.2×10^{17}
255	0.40 ± 0.01	0.20	13.8	1.1×10^{18}
260	0.44 ± 0.02	0.14	14.8	5.2×10^{18}
270	0.45 ± 0.05	0.03	13.7	1.2×10^{18}
280	0.37 ± 0.02	0.20	12.6	2.0×10^{17}
285	0.37 ± 0.02	0.08	12.4	2.0×10^{17}
290	0.25 ± 0.02	0.23	9.5	2.4×10^{15}
295	0.23 ± 0.04	0.30	7.1	7.7×10^{13}
300	0.16 ± 0.06	0.81	10.0	2.5×10^{17}
		7-Azaindole		
250	0.059 ± 0.006	0.13	2.2	3.3×10^{10}
260	0.056 ± 0.001	0.11	2.6	4.8×10^{10}
270	0.058 ± 0.008	0.21	2.8	5.5×10^{10}
280	0.058 ± 0.006	0.07	2.8	6.7×10^{10}
290	0.039 ± 0.002	0.05	2.7	7.6×10^{10}
300	0.030 ± 0.005	0.24	2.4	5.3×10^{10}
310	0.026 ± 0.010	0.07	2.1	4.6×10^{10}
320	0.025 ± 0.007	0.25	1.4	1.7×10^{10}
		5-Methoxyindole		
240	0.27 ± 0.03	0.57	9.0	4.0×10^{14}
270	0.43 ± 0.02	0.17	9.9	1.2×10^{15}
300	0.25 ± 0.01	0.58	9.6	7.6×10^{14}
310	0.20 ± 0.02	0.74	9.8	5.1×10^{14}

[a] Fluorescence quantum yields are determined experimentally at 25 °C as described in the Experimental Section. [b] The quantum yield of photoionization, ϕ_{e^-}, and the Arrhenius activation energies and prefactors, E_a and A, are obtained from the temperature dependence of the fluorescence quantum yield at the indicated excitation wavelength, as described in the text. For simplicity, it is assumed that nonradiative processes such as intersystem crossing and internal conversion are independent of temperature and excitation wavelength. [c] The data for indole reveal an enormous variation in the value of the Arrhenius prefactor, A—a factor of 10^5. We are uncertain whether these results are an anomaly of the fitting procedure or whether real physical significance should be attributed to them. Arrhenius prefactors greater than 10^{13} s^{-1} are inconsistent with the nonradiative process in question being controlled by nuclear motions. Kirby and Steiner[27] have performed similar experiments for indole and obtain a prefactor of 2.5×10^{16} s^{-1}. They do not, however, indicate their excitation wavelength. An unusually large prefactor may be a result of not fitting the data over a wide enough range of temperatures, or it may reveal an inappropriate form for the temperature dependence of the rate. Frauenfelder and co-workers have commented on large prefactors for the rates of ligand binding to myoglobin.[62]

$$\phi_F(\lambda) = \int_0^\infty (1.0 - \phi_{e^-}(\lambda))F(t)dt \qquad (4)$$

For a two-level system characterized by emitting ^1L_b and ^1L_a states,[41,42] the fluorescence decay is given by $F(t) = \alpha_1 \exp(-t/\tau_1) + \alpha_2 \exp(-t/\tau_2)$. If $\tau_2 \gg \tau_1$, then the fluorescence quantum yield is determined only by the long-lived component, and $\phi_F(\lambda) = [1.0 - \phi_{e^-}(\lambda)]k_R\tau_2$, where k_R is the radiative rate of the fluorescent species. Our measurements in water indicate that the radiative rate, k_R, is 1.05×10^8 s^{-1} for indole; 3.3×10^7 s^{-1}, for 7-azaindole; and 1.07×10^8 s^{-1}, for 5-methoxyindole. We define $y_0 = 1.0 - \phi_{e^-}(\lambda)$ and $\tau_2 = (k_R + k_0 + k(T))^{-1}$, where for simplicity we have assumed that *there is only one temperature-dependent nonradiative process, $k(T)$*, and only one temperature-independent nonradiative process, k_0, such as intersystem crossing.[5,26,58] We have set k_0 equal to the rate for intersystem crossing, 3.3×10^7 s^{-1}. If $k(T) = A \exp(-E_a/RT)$,

$$\phi_F^{-1}(\lambda) = A_0 + A_1 \exp(-E_a/RT) \qquad (5)$$

where

$$A_0 = \frac{1}{y_0} + \frac{k_0}{y_0 k_R} \text{ and } A_1 = \frac{A}{y_0 k_R}$$

Plotting the experimental data as $\phi_F^{-1}(\lambda)$ vs $1/T$ yields an exponential plus a background from which we may obtain A_0, A_1, and E_a (Figure 7a, Table 4). A similar analysis has been performed by Kirby and Steiner.[27] Knowledge of k_R and k_0 permits the determination of y_0 and, consequently, ϕ_{e^-}. Similarly, the activation parameters obtained from the fit permit the determination of the fluorescence lifetime, $\tau_F = \tau_2$, at any temperature

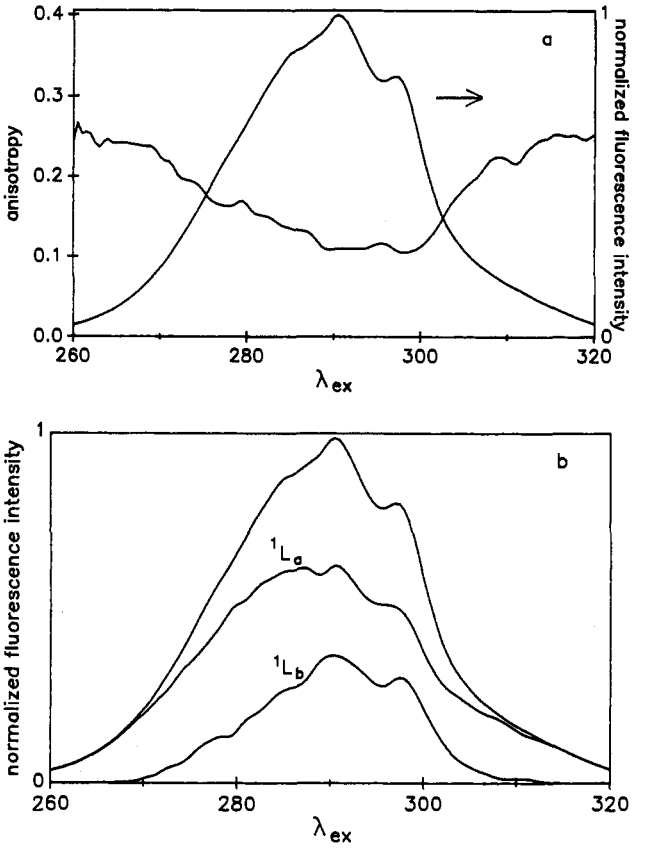

Figure 6. (a) The excitation anisotropy of 7-azaindole (7AI) (λ_{em} = 372 nm). (b) The corrected excitation spectrum of 7AI resolved into contributions from the ^1L_a and ^1L_b bands. $r_{oa} = 0.25$ and $r_{ob} = -0.13$. See ref 3 for a discussion of this analysis.

$$\tau_F = [k_R + k_0 + A \exp(-E_a/RT)]^{-1} \qquad (6)$$

The self-consistency of this approach is demonstrated by the comparison of the measured fluorescence lifetimes (Figure 7b) and the fluorescence lifetimes obtained from the temperature-dependent quantum yield data (see below).

It is significant that one exponential is sufficient to describe the temperature dependence of the steady-state data in water (Table 4, Figure 7). We find that the Arrhenius parameters obtained from the temperature dependence of the fluorescence lifetimes in water are newly identical to those obtained from the fluorescence quantum yields: indole (λ_{ex} = 288 nm), E_a = 9.3 kcal/mol, $A = 1.2 \times 10^{15}$ s^{-1}; 7-azaindole (λ_{ex} = 285 nm), E_a = 2.4 kcal/mol, $A = 7.3 \times 10^{10}$ s^{-1}; 5-methoxyindole (λ_{ex} = 288 nm), E_a = 7.8 kcal/mol, $A = 6.1 \times 10^{13}$ s^{-1}.

Because the fluorescence detected in our experiments is collected after the photoionization event, and because the steady-state and the time-resolved measurements yield identical activation energies, we conclude that the majority of photoelectrons are produced by means of a temperature-independent pathway and that the observed activation energies reveal the presence of another nonradiative process that is thermally activated. The photoelectrons are most likely produced by a temperature independent pathway, such as tunnelling. It is possible, however, that thermal activation of the "fluorescent" state produces solvated electrons with the reported activation parameters. The yield of solvated electrons from the "fluorescent" state is not expected to be more than 10% of that produced instantaneously from the Franck–Condon region (Figure 3b).

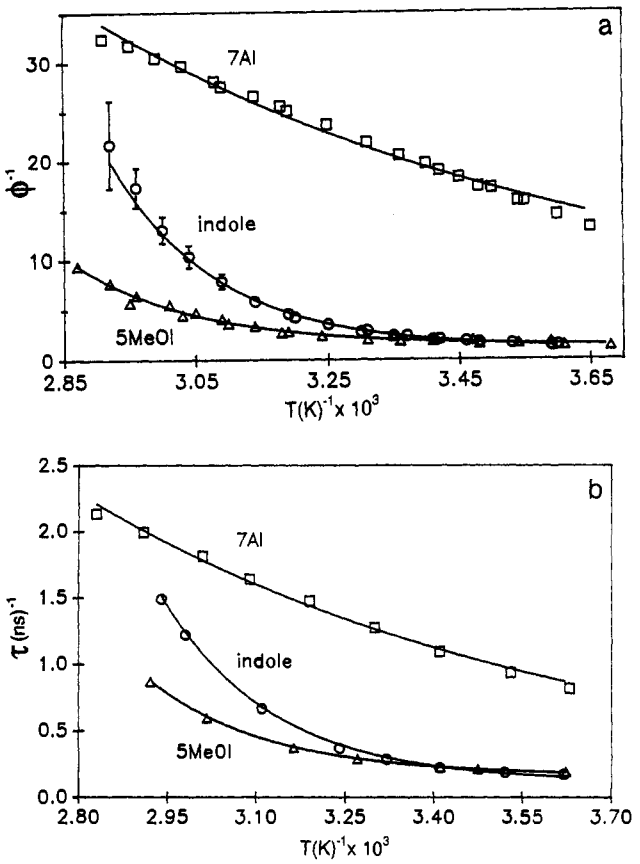

Figure 7. (a) Plots of ϕ_F^{-1} vs T^{-1} for indole, 7-azaindole, and 5-methoxyindole at neutral pH. The plots are presented for only one excitation wavelength for each molecule: indole, λ_{ex} = 285 nm; 7-azaindole, λ_{ex} = 290 nm; 5-methoxyindole, λ_{ex} = 285 nm. In general, within experimental error (Table IV) identical Arrhenius parameters are obtained for a given molecule at all excitation wavelengths. The only difference in the data is that the plots are displaced along the ordinate owing to the excitation-wavelength dependence of the fluorescence quantum yield. (b) Plots for indole, 7-azaindole, and 5-methoxyindole at neutral pH obtained from the inverse of the fluorescence lifetimes (less the temperature-independent rates) using an excitation wavelength of 285 nm.

Lee and Robinson[63] have performed an interesting, detailed, and original analysis of the nonradiative processes of indole in water/methanol mixtures using fluorescence lifetime and fluorescence quantum yield measurements. It is useful to compare and contrast our results and conclusions with theirs. Because of the agreement between lifetime measurements obtained with a neodymium/phosphate-glass laser and quantum yield measurements, they conclude that the nonradiative processes they observe result from monophotonic events. By analogy with previous work on photoionizing compounds such as anilino/naphthalene sulfonic acid (ANS)[64] and from evidence in the literature indicating that indole produces photoelectrons, Lee and Robinson *assume* that the nonradiative process measured in their experiments is photoionization. Since they do not directly monitor absorption from the solvated electron, their assignment of the nonradiative process is tentative. As we note in the previous paragraph and elsewhere in this article, we can never observe more than 10% of a contribution of solvated electron whose rise time coincides with the decay time of the fluorescent state. Below we suggest the importance of abstraction of the N_1 proton in deactivating the fluorescent state. Regardless of the identity of the nonradiative process for indole observed in the experiments of Lee and Robinson, it is clear that it is very sensitive to solvent. For example, from the temperature dependence of the nonradiative rate they obtain activation energies of 10.4 and ~0.0 kcal/mol in water and methanol, respectively.[63] Assuming that the nonradiative process is photoionization, Lee and Robinson suggest that in methanol trapping of the photoelectron by a solvent cage is unfavorable and that a rapid recombination occurs that reforms ground-state indole. The optimum cage is proposed to be formed from about four water molecules.[63] With regard to our photoionization measurements of 7-azaindole, the electron yield in water is greater by about a factor of 2 than that in methanol. If this reduction in yield results from recombination with the parent cation, the back reaction must occur in <1 ps (beyond our time resolution). We observe no geminate recombination 150 ps subsequent to photoionization.[8] Similarly, for indole in butanol, no recombination is observed on the 30-ps time scale investigated subsequent to photoionization.[8]

Our conclusions are in contrast to those of Feitelson[25] and Bent and Hayon,[7] which have significantly influenced the interpretation of indole photophysics over the past 20 years. Feitelson proposed that the production of photoelectrons from indole was temperature dependent based on indirect measurements of hydrogen evolution. Bent and Hayon performed direct flash photolysis measurements of the solvated electron. They observed that the optical density change, ΔA, at 650 nm due to the solvated electron produced from indole at pH 7.5 is temperature dependent. Figure 4 of their article presents these raw data. A plot of ΔA vs $1/T$ yields an apparent activation energy of 0.37 kcal/mol. A plot of $\ln(\Delta A)$ vs $1/T$ yields an apparent activation energy of 4.9 kcal/mol, when the absorbance data have been corrected for the shift of the spectrum of the solvated electron with temperature.[28] The interpretation of these results is not straightforward. The quantum yield of photoelectrons is, by definition

$$\phi_{e^-} = \frac{k_{e^-}}{k_{e^-} + \sum_i k_i} \tag{7}$$

where the k_i represent all the other processes, radiative and nonradiative, that deactivate the excited state. ϕ_{e^-} is proportional to k_{e^-} only if $k_{e^-} < \sum_i k_i$; this is unlikely since in 7-azaindole the solvated electron appears in ≤130 fs[8] and, in every other example studied here, within a 1-ps pulse width. It is therefore inappropriate to attach any physical significance to the activation energies obtained from the temperature dependence of the absorbance change resulting from the solvated electron.

The temperature dependence observed by Bent and Hayon for the electron yield may be attributed to changes in the ground-state absorption spectrum with temperature. As can be seen for indole in Figure 8, raising the temperature decreases the shoulder at 290 nm and increases the absorbance in the short-wavelength region of the spectrum. Such a temperature-dependent absorption increase occurs at 265 nm, the excitation wavelength used by Bent and Hayon. The increase in electron yield that they report may thus be attributed to shifts in the spectra resulting from the $^1A \rightarrow {}^1L_a$ and $^1A \rightarrow {}^1L_b$ transitions.

If the observed activation energy in indole derivatives does not reflect thermally activated photoionization, what nonradiative process is involved? Glasser and Lami[29] have proposed that in the vapor-phase dissociation of the N–H bond is an important nonradiative process. Detailed information on the ^1L_a and ^1L_b states in jet-cooled indoles has become accessible.[30-36] Wallace and co-workers[35] undertook an investigation of 2,3-dimethylindole, which is known to have a low-lying ^1L_a state in all media.[37] Their work yielded evidence that the ^1L_b state was *strongly coupled* to the ^1L_a state, from which dissociation of the N–H bond could occur. These results deal with site-specific hydrogen-bonding interactions in the gas phase. We have performed[38] proton inventory experiments[39] of 7-azaindole in water and have suggested that abstraction of the N_1 hydrogen may be an important,

(62) Frauenfelder, H.; Sligar, S. G.; Wolynes, P. G. *Science* **1991**, *254*, 1598.
(63) Lee, J.; Robinson, G. W. *J. Chem. Phys.* **1984**, *81*, 1203.
(64) Drew, J.; Thistlethwaite, P.; Woolfe, G. *Chem. Phys. Lett.* **1983**, *96*, 296. Sadkowski, P. J.; Fleming, G. R. *Chem. Phys.* **1980**, *54*, 79. Moore, R. A.; Lee, J.; Robinson, G. W. *J. Phys. Chem.* **1985**, *89*, 3648. Lee, J.; Robinson, G. W. *J. Am. Chem. Soc.* **1985**, *107*, 6153.

temperature-dependent, nonradiative process in indoles, especially 7-azaindole. Barkley and co-workers[40] have recently discussed hydrogen abstraction as a possible nonradiative pathway in indoles.

We suggest that the excitation-wavelength dependence of the fluorescence quantum yield reflects the coupling (most likely vibronic, see below) of the zero order ^1L_a and ^1L_b states. These results argue against the utility of using zero-order pictures of ^1L_a and ^1L_b states to describe the photophysics of indole and its derivatives. Similar conclusions have been obtained by Wallace and co-workers[35] and Fleming and co-workers.[12]

B. The Effect of Closely-Spaced Excited States. First Cross et al.[41] and then Szabo[42] demonstrated how the presence of two excited electronic states whose energy gap is close to kT can influence the short time anisotropy decay and hence give rise to apparently anomalously low $r(0)$ values if the anisotropy measurement is not performed with sufficient time resolution. Subsequently, Fleming and co-workers[12,43] experimentally observed these effects. Subpicosecond resolution reveals $r(0) = 0.4$ and rapid components of the anisotropy decay in the range of 1–4 ps.

In the specific case where there are two closely-spaced excited states, ^1L_a and ^1L_b, the measured anisotropy decay function is a function of both wavelength and time:[12,41]

$$r(\lambda,t) = \frac{k_R{}^a g^a(\lambda) r^a(t) K^a(t) + k_R{}^b g^b(\lambda) r^b(t) K^b(t)}{k_R{}^a g^a(\lambda) K^a(t) + k_R{}^b g^b(\lambda) K^b(t)} \quad (8)$$

where $k_R^{a,b}$ are the radiative rate constants, $K^{a,b}(t)$ are the population (fluorescence) decay laws, and $g^{a,b}(\lambda)$ are the emission line shapes, whose integrals are normalized to unity, of the ^1L_a and ^1L_b states. Thus, when two closely-spaced states can be reached from the ground state in an optical transition (or if the upper state can be thermally populated), the observed anisotropy decay is a superposition of the individual anisotropy decays. The form of the observed anisotropy decay will depend strongly on the extinction coefficient connecting the ground electronic state to ^1L_a or ^1L_b, which will determine $K^{a,b}(t = 0)$. The decay will also depend on the relative contribution of emission from the two states that is detected at a given wavelength.

Using the level scheme depicted in Figure 9, the following rate constants[12,41] are defined.

$$k^a = k^b = k_R^a + k_{NR}^a \quad (9)$$

Here we assume that $k_R^a = k_R^b$. We also assume that the sum of the rate constants of the nonradiative processes depleting ^1L_a and ^1L_b, neglecting internal conversion is the same for both levels: $k_{NR}^a = k_{NR}^b$. k_{ba} is the rate of ^1L_b to ^1L_a internal conversion. k_{ab} is the rate at which ^1L_b is thermally populated by ^1L_a and is determined using the appropriate ^1L_b–^1L_a energy gap and an estimated value of k_{ba}.

In order to evaluate the limiting anisotropies obtained from steady-state and time-domain measurements,[3] r_o and $r(0)$, respectively, we employ the following relationships.[44]

$$k^a(t) = \left(\frac{1}{2}Q\right)\{K^a(0)[Q - \delta] + 2k_{ba}K^b(0)\} \exp(l_1 t) + \left(\frac{1}{2}Q\right)\{K^a(0)[Q + \delta] - 2k_{ba}K^b(0)\} \exp(l_2 t) \quad (10)$$

$$K^b(t) = \left(\frac{1}{2}Q\right)\{K^b(0)[Q + \delta] + 2k_{ab}K^a(0)\} \exp(l_1 t) + \left(\frac{1}{2}Q\right)\{K^b(0)[Q - \delta] - 2k_{ab}K^a(0)\} \exp(l_2 t) \quad (11)$$

$$\delta = k^a + k_{ab} - k^b - k_{ba} \quad (12)$$

$$Q = [\delta^2 + 4k_{ab}k_{ba}]^{1/2} \quad (13)$$

$$k = k^a + k_{ab} + k^b + k_{ba} \quad (14)$$

Table 5. Comparison of Initial $^1L_a/^1L_b$ Populations for Tryptophan Obtained from Measurements of Fluorescence and Anisotropy Decay[a]

λ_{ex}[b] (nm)	α_1	α_2	α_1/α_2	$K^b(0)$	$K^b(0)^{r(t)}$
305	0.77	0.23	3.35	0.43	0.01
303	0.66	0.34	1.94	0.70	0.03
300	0.69	0.31	2.23	0.62	0.05
297	0.65	0.35	1.86	0.72	0.11
294	0.59	0.41	1.44	0.92	0.16
292	0.59	0.41	1.44	0.92	0.18
290	0.77	0.23	3.35	0.43	0.40

[a] α_1 and α_2 are the experimentally determined preexponential factors for the excited-state population (fluorescence) decay obtained by Fleming and co-workers[12] with subpicosecond resolution. $K^b(0)$ is the initial relative population of the ^1L_b state predicted from their reported values of α_1 and α_2 by eqs 18 and 19. The last column labeled $K^b(0)^{r(t)}$ is the initial relative population of the ^1L_b state required by Fleming and co-workers to fit their experimental anisotropy decay. [b] In each case λ_{em} = 335 nm.

$$l_1 = -\frac{1}{2}(k - Q) \quad (15)$$

$$l_2 = -\frac{1}{2}(k + Q) \quad (16)$$

We can express the total fluorescence decay as contributions from both the ^1L_b and ^1L_a states.

$$K(t,\lambda) = g^a(\lambda)K^a(t)k_R + g^b(\lambda)K^b(t)k_R \quad (17)$$

and we assume as before that $k_{NR}^a = k_{NR}^b = k_R$. Inserting eqs 14 and 15 into the above expression, we obtain

$$K(t) = \frac{k_R}{2Q}[g^a(\lambda)K^a(0)(Q - \delta) + 2g^a(\lambda)k_{ba}K^b(0) + g^b(\lambda)K^b(0)(Q + \delta) + 2g^b(\lambda)k_{ab}K^a(0)] \exp(l_1 t) + \frac{k_R}{2Q}[g^a(\lambda)K^a(0)(Q + \delta) - 2g^a(\lambda)k_{ba}K^b(0) + g^b(\lambda)K^b(0)(Q - \delta) - 2g^b(\lambda)k_{ab}K^a(0)] \exp(l_2 t) \equiv \alpha_1 \exp(-t/\tau_1) + \alpha_2 \exp(-t/\tau_2) \quad (18)$$

The total fluorescence decay is described by a double exponential with prefactors α_1 and α_2. The prefactors contain the values of the population of the ^1L_a and ^1L_b states at time zero, $K^a(0)$ and $K^b(0)$. Fleming and co-workers[12] have measured these prefactors for tryptophan under various conditions of excitation and detection with subpicosecond resolution. If we assume,[57] as they do, that the relative intensities of the ^1L_a and ^1L_b emission are $g^a(\lambda) = 0.35$ and $g^b(\lambda) = 0.65$ and that $k_{ba} = 0.625$ and $k_{ab} = 0.044$ ps^{-1}, we can work backwards from their experimentally determined preexponential factors for the population decay and solve for $K^a(0)$ and $K^b(0)$:

$$\frac{\alpha_1}{\alpha_2} = \frac{g^a(\lambda)K^a(0)(Q - \delta) + 2g^a(\lambda)K^b(0)k_{ba} + g^b(\lambda)K^b(0)(Q + \delta) + 2g^b(\lambda)K^a(0)k_{ab}}{g^a(\lambda)K^a(0)(Q + \delta) - 2g^a(\lambda)K^b(0)k_{ba} + g^b(\lambda)K^b(0)(Q - \delta) - 2g^b(\lambda)K^a(0)k_{ab}} \quad (19)$$

The initial populations obtained from subpicosecond anisotropy and fluorescence decay measurements are summarized in Table 5. In every case, the result of the lifetime measurement indicates a much larger ^1L_b population than would have been obtained from a consideration of only the anisotropy measurement. It is this discrepancy that we address in the next section.

C. Modeling Anisotropy Data (Inclusion of Photoionization at "Zero Time"). We have collected a large body of data on the monophotonic, instantaneous ionization of 7-azaindole, indole, and their derivatives and demonstrated that this ionization is excitation-wavelength dependent. We have also observed that the ^1L_a state is preferentially and *dynamically* solvated with respect to higher excited states in 7-azaindole.[8] This assignment

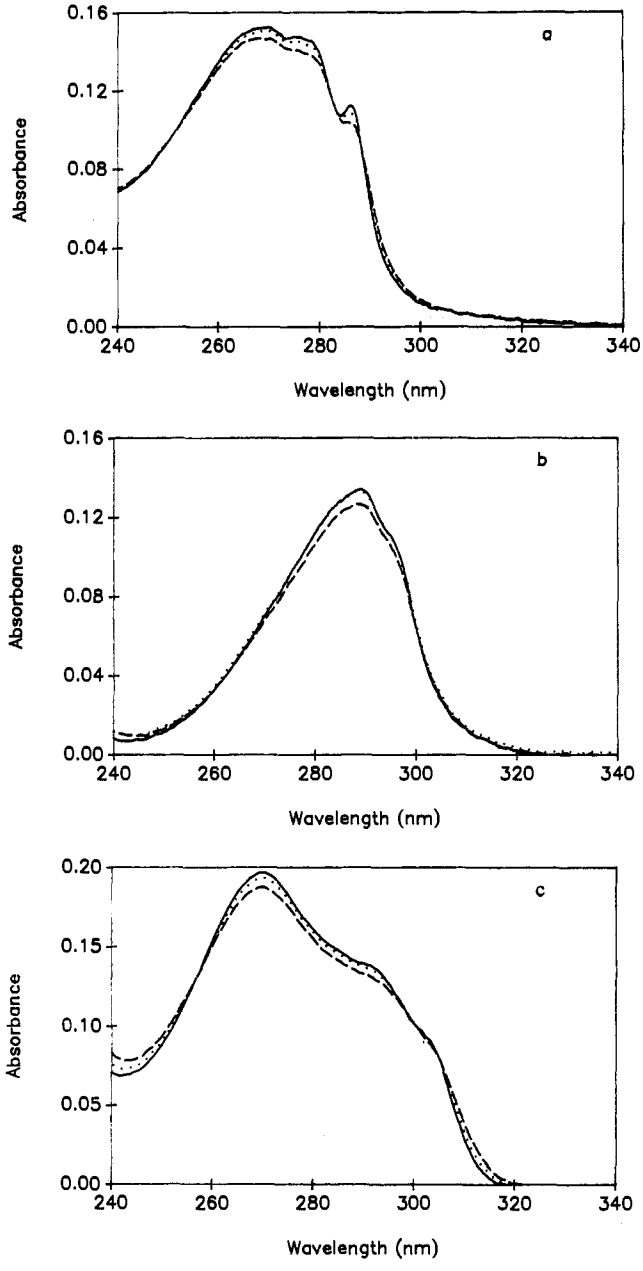

Figure 8. Temperature dependence of the absorption spectrum of the ground-state of indole derivatives: (a) indole, (b) 7-azaindole, (c) 5-methoxyindole, 10 °C (—), 40 °C (···), 79 °C (– –). The change in absorption spectra with temperature is suggested to explain the temperature dependence of the electron yield observed by Bent and Hayon.[7]

is based on the observation of preferential solvation of the ^1L_a state in polar media.[45] In the following, we incorporate these factors into the description of the anisotropy decay of indole and demonstrate that the observations presented in this article are consistent with the early-time anisotropy decay measurements[12,43] (Figure 9).

We tentatively attribute the photoionization to ^1L_b for the following reasons.

1. The quantum yields for fluorescence and photoionization are excitation-wavelength dependent (Figure 6 and Tables 2 and 4). If both states were photoionizable, the excitation-wavelength dependence would be expected to be much weaker or absent.

2. In 5-methoxyindole, ^1L_b is the lowest excited singlet.[10] 5-Methoxyindole also possesses one of the largest ^1L_b–^1L_a energy gaps among the indoles. Because the solvated electron appears within 1 ps for excitation wavelengths as red at 305 nm for 5-methoxyindole, it is clear that ^1L_b is photoionizable.

We propose that most of the photoionization occurs only at the moment of excitation, that is, immediately upon excitation, or at

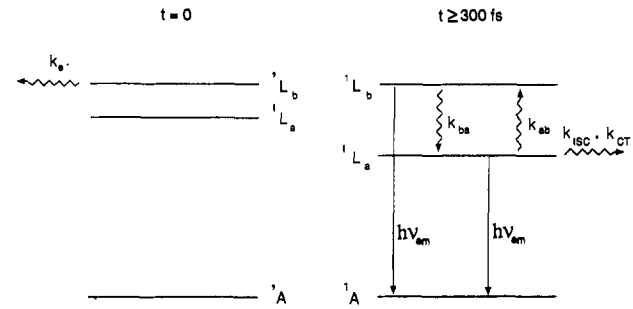

Figure 9. Energy level diagram. The scheme is modified from that of Cross et al.[41] in order to take into account ionization from the ^1L_b state. ^1L_b is believed to lie slightly (~500 cm^{-1}) above ^1L_a in indole. The ^1L_b–^1L_a energy gap is expected to be small in 7-azaindole based on its lower steady-state anisotropy values. In 5-methoxy- and 5-hydroxyindole, ^1L_b is believed to lie below ^1L_a, with a significant energy gap, based on steady-state anisotropy data.[10] We have demonstrated that there is excited-state dynamic solvation of 7-azaindole. This occurs in ~300 fs in methanol. We attribute this solvation to the ^1L_a state and schematically indicate its position at $t = 0$ and at a later time when excited-state solvation is accomplished. The ^1L_b level is shown to photoionize only on the left-hand side of the figure (i.e., at $t = 0$), because our results indicate that *most of the photoionization occurs at this time.* After the initially prepared population has moved out of the Franck–Condon region and into the right-hand side of the figure, other nonradiative processes become significant. (The most cogent evidence for the basic validity of the level kinetics model[41,42] is the observation of the rise time in the time-resolved fluorescence anisotropy.[12] This rise time is controlled by the rate of population of the upper state by the lower state k_{ab}.

$t = 0$.[8] *At subsequent times, the initially prepared wavepacket will be displaced, and photoionization will no longer be possible.* Furthermore, at subsequent times, for indole, 7-azaindole, and their derivatives, the ^1L_a state will be stabilized or solvated with respect to the ^1L_b state. This preferential solvation event occurs in ~300 fs for 7-azaindole in methanol.[8]

If for λ_{ex} = 305 nm at $t = 0$ the initial populations in the ^1L_b and ^1L_a levels are $K^b(0) = K^a(0) = 0.5$ and $\lambda_{e^-} = 0.3$ (Table 5), the populations at a *later* time, $t \sim 0$, must be correspondingly diminished by the depletion produced by photoionization. Thus at a later time, the normalized populations are $K^b(t \sim 0) = 0.2/0.7 = 0.28$ and $K^a(t \sim 0) = 0.5/0.7 = 0.72$. At λ_{ex} = 300 nm where $\phi_{e^-} = 0.4$, the corresponding populations are $K^b(t \sim 0) = 0.17$ and $K^a(t \sim 0) = 0.83$. Given the resolution of any currently realizable time-resolved experiment, these residual populations not depleted by photoionization are in fact taken as the zero time populations measured in steady-state experiments or by time-correlated single-photon counting.

Figure 10 presents the anisotropy decay data of Fleming and co-workers for tryptophan at λ_{ex} = 305 and 300 nm. Superimposed on their results are our simulations using the zero time populations of the ^1L_b and ^1L_a states corrected for photoionization. Our simulation is identical with the global fit to the experimental data when noise is taken into account.

The important conclusion to be drawn from this exercise is that the amount of the ^1L_b excited-state population in indole, 7-azaindole, and their derivatives that possess small ^1L_b–^1L_a energy gaps is more than that estimated from subpicosecond *anisotropy decay* measurements or from steady-state anisotropy measurements. We have discussed this point elsewhere.[3] The agreement of the zero time populations of our simulation with those obtained from the subpicosecond *lifetime* measurements[12] (Table 5) illustrates this point.

Crucial to our analysis are the observations that the solvated electron is produced instantaneously (<1 ps) and that the fluorescence quantum yield is also excitation-wavelength dependent for molecules whose lowest lying excited state is believed to be ^1L_b and in which there is a relatively large ^1L_b–^1L_a energy gap: 5-methoxy- and 5-hydroxyindole.

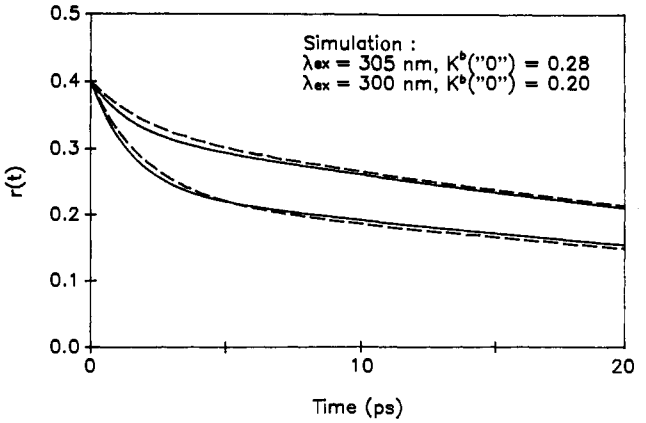

Figure 10. Comparison of the global fit (– –) of the subpicosecond fluorescence anisotropy data for tryptophan of Fleming and co-workers[12] with a simulation (—) taking into account "zero time populations" of the ^1L_a and ^1L_b states that are corrected for photoionization. As we discuss in the text, "zero time" refers to the population of the excited states that *remains* after the instantaneous photoionization event. The figure indicates that we are able to simulate very well the results of Fleming and co-workers by using ^1L_b populations at "zero time" of 0.28 and 0.20 at excitation wavelengths of 305 and 300 nm, respectively. At 300 nm, we use $K^b(0) = 0.20$ instead of 0.17 because it gives better agreement with the experimental data and because 0.20 is within the bounds of experimental error in our electron yield measurements (Table II). The ^1L_b populations that we estimate from our electron yield measurements are significantly larger than the populations required to fit *globally* the experimental anisotropy decay data and are closer to the populations obtained from the global analysis of the experimental population decay data (Table V).

Based on these observations, we have assigned the ^1L_b state as the origin of the solvated electron at $t = 0$. In indole and 7-azaindole, where ^1L_a is lower lying but where the energy gap is much smaller (based on fluorescence anisotropy measurements), we suggest that ^1L_a is capable of photoionization as long as it is coupled to ^1L_b. As the ^1L_a state is preferentially solvated this coupling will decrease and this state, giving rise to fluorescence in steady-state and conventional time-correlated single-photon counting measurements, will no longer be a source of solvated electrons (Figure 9).

Conclusion

The description of the excited states of indole, 7-azaindole, and their derivatives proposed above is useful insofar as it can be used to explain or at least to rationalize the photophysics of more complex molecules—among which is the naturally occurring amino acid, tryptophan. Essentially all tryptophan derivatives and peptides bearing *nonrigid* side chains display nonexponential fluorescence decay.[6,48,49] A notable exception is *N*-acetyltryptophanamide (NATA), which affords a single exponential fluorescence decay of about 3 ns at 20 °C.[6] 5-Hydroxytryptophan has also been observed to have a single-exponential fluorescence decay;[50] we have measured its lifetime at 20 °C and neutral pH to be 3.8 ns.

We have suggested that this nonexponential fluorescence decay arises from two (or more) side-chain orientations with respect to the indole moiety. Each orientation is characterized by a different rate of charge transfer from the indole donor to the side-chain acceptor.[6] The existence of stable conformational isomers (conformers) of tryptophan is supported by NMR data.[49,51] Molecular dynamics simulations of Engh et al.[52] have suggested different stable conformations between the indole ring and the side chain in tryptophan. Levy and co-workers[30-33] have observed different conformers of tryptophan and tryptophan-containing compounds in supersonic jets.

The fluorescence decay of zwitterionic tryptophan is fit well to two exponentially decaying components, namely to the function[6] $K(t) = 0.22 \exp(-t/620 \text{ ps}) + 0.78 \exp(-t/3200 \text{ ps})$. Measurement of the lifetime as a function of emission wavelength reveals that the short-lived component is blue-shifted with respect to the

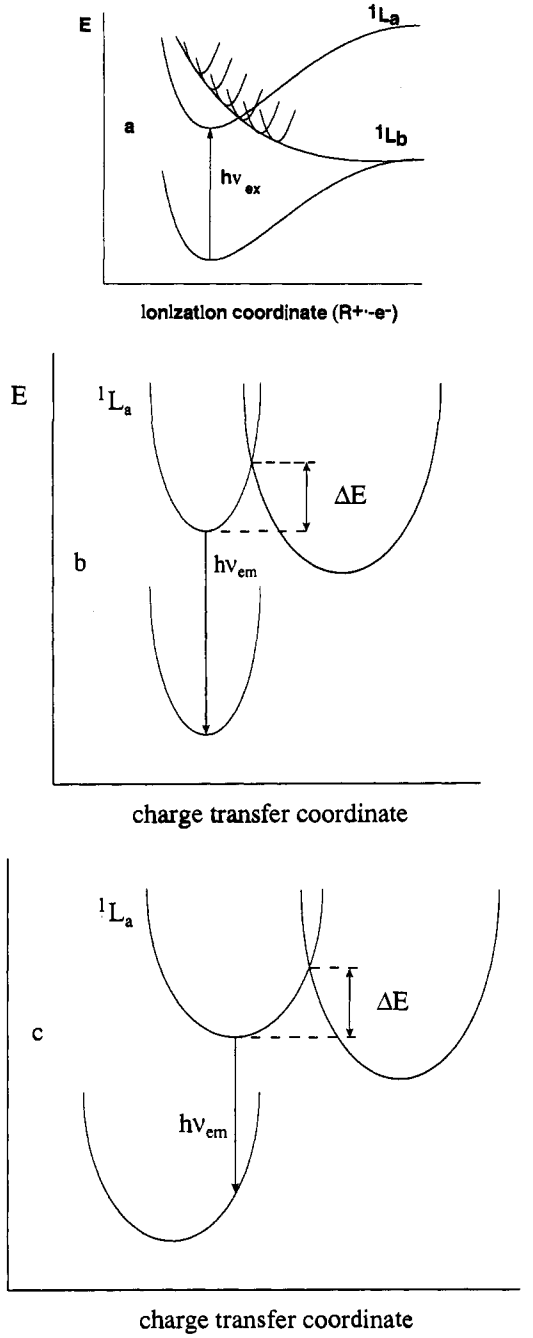

Figure 11. Potential energy diagrams of indole derivatives as a function of two coordinates. (a): The ^1L_b surface is proposed to be dissociative in one coordinate and bound in the other(s). The bound character of the ^1L_b surface is indicated by the sequence of parabolas tangent to it. Upon light absorption, the initially prepared wavepacket has either "slid down" the dissociative surface, producing the radical cation and the solvated electron, or "spilled out" into an orthogonal coordinate. (b) and (c): The ^1L_a surface of tryptophan is proposed to be coupled to a charge-transfer coordinate that involves the amino acid side chain. It is suggested that in certain conformers, this coordinate has a higher frequency than in others (b as opposed to c, for example) and thus manifests a larger rate of charge transfer to the side chain. The barrier to charge transfer is set equal in each case since it is known that in zwitterionic tryptophan the activation barrier is the same for each of the two exponentially decaying components.[6] Finally, it is known that the short-lived (620 ps) component is blue-shifted with respect to the long-lived (3200 ps) component in zwitterionic tryptophan. These spectral shifts are depicted schematically in the figure. By side-chain coordinate we refer to all contributions to the reaction coordinate involved in the charge-transfer reaction. The most significant component is obviously the amino acid side chain itself, but the contribution from the solvent cannot be neglected.

long-lived component.[6,53] The two components obtained in the fluorescence decay of zwitterionic tryptophan and essentially all tryptophan analogs and tryptophan-containing peptides have temperature dependencies that yield identical Arrhenius activation energies, E_a, but different Arrhenius prefactors.[6]

Figure 11 provides a means of summarizing the data presented in this article on the photoionization of the excited states of indoles and also provides a qualitative explanation of the nonexponential fluorescence decay kinetics of zwitterionic tryptophan. Figure 11 considers the indolyl photophysics in the context of a three-dimensional energy surface. The energy is a function of an ionization coordinate determined by an $R^{\bullet+}$–e^- distance and a charge-transfer-to-side-chain coordinate. The body of data on indole and its derivatives can be rationalized by taking the ^1L_b surface to be highly asymmetric in two coordinates and by using propagating wavepackets[54] to describe excited-state dynamics. Comparison of Figure 11a,b shows the ^1L_b surface to be dissociative in the ionization coordinate and bound in the side-chain or charge-transfer coordinate.

In indole and 7-azaindole derivatives, because ^1L_a and ^1L_b lie so close to one another, upon light absorption significant populations of each are excited (Table 5, Figures 9 and 11). The wavepacket projected onto the ^1L_b surface can either slide down the dissociative chute along the ionization coordinate (Figure 11a) or spill over into the ^1L_a surface if the ^1L_a surface crosses the ^1L_b surface near its minimum (Figure 11b). Thus, about a femtosecond after excitation, the initially prepared population is either photoionized or localized in bound states. This time corresponds to the inverse bandwidth[54] of the indole absorption spectrum.

Fluorescence measurements performed with steady-state or time-correlated, single-photon counting apparatus will only probe areas of the potential energy surfaces illustrated in Figure 11b,c owing to their limited time resolution. The regions of the potential surface displayed in Figure 11b,c are no longer susceptible to instantaneous ionization. It is known, however, that the presence of electrophilic side-chain groups in tryptophan induces nonexponential fluorescence decay from, presumably, the ^1L_a state. The activation barrier for this process is determined by the intersection of the surface for the charge-separated state with that of the ^1L_a state. If there is a distribution of ^1L_a states with different frequencies for the side chain mode, it is possible to obtain crossings between the ^1L_a and the charge-separated states that all possess the same activation barrier (Figures 11b,c). The rate of passage from ^1L_a to the charge-separated state will now be determined by the curvature[55] of the ^1L_a surface. The larger the curvature or the higher the frequency of the side-chain mode, the larger the rate for the charge-transfer process.

The absence of nonexponential fluorescence decay in NATA may now be explained if all its conformers have similar side-chain frequencies and intersect the charge-separated surface at the same position. The absence of nonexponential fluorescence decay in 5-hydroxytryptophan, where ^1L_b is the fluorescent state, can be attributed to a much higher barrier crossing between the ^1L_b and the charge-separated states.

For tryptophan at high pH, the carboxylic acid is deprotonated, and the amino group is uncharged; hence, neither group is a good charge acceptor,[6] the fluorescence lifetime becomes insensitive to the side chain distribution, and single exponential fluorescence decay arises.[6] We observe a finite rise time of ~3 ns for the appearance of the 10% of the solvated electron produced at pH 12.3 in tryptophan (Figure 4b). This rise time corresponds to the 3.2-ns fluorescence decay at pH 12.3. Similarly, Bent and Hayon[7] observe about 10% of the solvated electron produced at pH 10.3 in tryptophan to appear with an ~8-ns time constant. Again, this rise time agrees with the fluorescence decay time of the anionic tryptophan. An explanation for this behavior is that when the charge-transfer states are no longer accessible at high pH, thermal activation can transfer population from the ^1L_a state back to the dissociative ^1L_b surface. Instantaneous rise times for the solvated electron are observed at high pH for 5-hydroxytryptophan and all other compounds investigated here. In 5-methoxy- and 5-hydroxyindole and 5-hydroxytryptophan, the ^1L_b state is the lowest and hence is the fluorescent state.

Zwitterionic 7-azatryptophan is expected to have the same distribution of conformers in aqueous solution as zwitterionic tryptophan; and although zwitterionic 7-azatryptophan has its ^1L_a state lying slightly below its ^1L_b state,[3] it is characterized by a single exponential fluorescence decay over most of the pH range when emission is collected over most of its band.[1,2,5] This distinguishing characteristic of 7-azatryptophan, which contributes greatly to its amenability as a fluorescent probe,[1,4] shall be discussed elsewhere.

Acknowledgment. This work was partially supported by the ISU Biotechnology Council, University Research Grants, and IPRT. J.W.P. is an Office of Naval Research Young Investigator. F.G. is the recipient of a fellowship from Phillips Petroleum. R.L.R. is a GAANN fellow.

(65) Orstan, A.; Ross, J. B. A. *J. Phys. Chem.* **1987**, *91*, 2739.
(66) Chen, R. F. *Anal. Biochem.* **1967**, *19*, 374.
(67) Berlman, I. B. *Handbook of Fluorescence Spectra of Aromatic Molecules*; Academic Press: New York and London, 1971.
(68) Parker, C. A. *Photoluminescence of Solutions*; Elsevier Publishing Company: Amsterdam, 1968.
(69) Morris, J. V.; Mahaney, M. A.; Huber, J. R. *J. Phys. Chem.* **1976**, *80*, 969.
(70) Kaye, G. W. C.; Laby, T. H. *Table of Physical and Chemical Constants*; Longman Group Limited: London, 1973.